Title: The Effect of Adding Rubber Crumbs on the Cyclic Permanent Deformation of Waste Mixtures Containing Coal Wash and Steel Furnace Slag

Author 1

- Yujie Qi, PhD, MSc, BSc,
- Lecturer, & Program Co-leader of Transport Research Centre, Faculty of Engineering and Information Technology, University of Technology Sydney, NSW 2007, Australia
- https://orcid.org/0000-0002-3486-2130

Author 2

- Buddhima Indraratna, PhD (Alberta), MSc and BSc-Hons (London), FTSE, FIEAust, FASCE, FGS, FAusIMM, FIES, DIC, CEng, CPEng;
- Distinguished Professor of Civil Engineering, Founding Director of Australian Research Council's Industrial Transformation Training Centre for Advanced Technologies in Rail Track Infrastructure (ITTC-Rail), Director of Transport Research Centre, School of Civil and Environmental Engineering, University of Technology Sydney, NSW 2007, Australia
- https://orcid.org/0000-0002-9057-1514

***Author for correspondence:**
Distinguished Prof. Buddhima Indraratna
Director, Transport Research Centre,
Faculty of Engineering and Information Technology,
University of Technology Sydney
Email: buddhima.indraratna@uts.edu.au

Abstract

Among the numerous studies into the dynamic loading behaviour of rubber crumbs-soil/waste mixtures, the main focus is on how the content of rubber crumbs (R_b%) affects the damping ratio, shear modulus and total deformation. However, the research into the influence of R_b% on the permanent strain rate ($\dot{\varepsilon}_p$) and the deformation mechanism under repeated loading is very limited. In this current study, the cyclic deformation response for the waste mixtures of steel furnace slag (SFS), coal wash (CW) and rubber crumbs (RC) are analysed and the test results reveal that R_b% has a significant influence on the initial $\dot{\varepsilon}_p$ and the slope of the permanent axial strain rate line (PASRL), while cyclic deviator stress ($q_{cyc,max}$) mainly affects the initial $\dot{\varepsilon}_p$. The influence of R_b% and $q_{cyc,max}$ on $\dot{\varepsilon}_p$ of the waste mixture is incorporated in an empirical model, which enables to predict the permanent deformation mechanism of SFS+CW+RC mixtures with broader ranging amounts of RC and higher cyclic deviator stresses.

Keywords: repeated loading; deformation; strain; industrial wastes;

List of notations

α	is the the slope of the permanent axial strain rate line in $\log \dot{\varepsilon_p} - \log N$ space
β	the $\dot{\varepsilon}_p$ (the initial vertical strain) when N=1
ε_a	is the permanent axial strain
$\dot{\varepsilon}_p$	is the permanent strain rate
σ'_3	is the effective confining pressure
$q_{cyc,max}$	is the cyclic deviator stress
$q_{peak,static}$	is the peak deviator stress under static loading
R_b	is the content of rubber crumbs (%)
m, n	are empirical coefficients to determine α
A_1, A_2, B_1, B_2	are empirical coefficients to determine β
CW	is coal wash
CSR	is the cyclic stress ratio
N	is the number of loading cycles
PASRL	is the permanent axial strain rate line
RC	is rubber crumbs
RCA	is recycled concrete aggregates
SFS	is steel furnace slag

Introduction

When granular materials are subjected to cyclic loading, the vertical deformation response can be divided distinctly into the resilient and the permanent components. The excessive permanent vertical deformation is one of the main factors that lead to the failure of a roadway or track over a large number of cycles albeit the incremental vertical deformation for each loading cycle (permanent vertical strain rate; $\dot{\varepsilon}_p$) is usually very small. To characterize the permanent deformation behaviour of granular materials subjected to repeated loading, $\dot{\varepsilon}_p$ is usually taken as the main indicator for different patterns of the deformation mechanism. Previous studies (e.g. Li and Selig, 1996; Wichtmann *et al.*, 2007; Cerni *et al.*, 2012; Sun *et al.*, 2015; Saberian *et al.*, 2018) indicated that $\dot{\varepsilon}_p$ of granular materials is mainly affected by the type and physical state of the soil and stress state. However, the influence of soil physical condition (e.g. density, water content) and stress state on $\dot{\varepsilon}_p$ have been investigated extensively (e.g. Tseng and Lytton, 1989; Saberian *et al.*, 2018; Cerni *et al.*, 2012; Monismith *et al.*, 1975; Li and Selig, 1996), whereas the influence of the soil type has not been studied in depth due to the complexity in the variety of soil, especially as marginal materials are becoming popular for dynamic loading projects.

In recent years, the use of rubber crumbs-soil/waste mixtures in rail tracks has been introduced due to the enhanced damping property and energy absorbing capacity of the mixture (Sol-Sánchez *et al.*, 2015; Esmaeili *et al.*, 2016; Fathali *et al.*, 2016; Indraratna *et al.*, 2017). For instance, Indraratna *et al.* (2017) developed a synthetic energy absorbing layer for railway subballast by mixing the waste materials together including steel furnace slag (SFS), coal wash (CW) and rubber crumbs (RC). The inclusion of RC can significantly affect the geotechnical properties of the RC-soil/waste mixtures, e.g. the shear strength, damping ratio, the critical state, the resilient modulus, and the overall deformation (Youwai and Bergado, 2003; Fu *et al.*, 2014; Mashiri *et al.*, 2015; Madhusudhan *et al.* 2017; 2019ab; Qi *et al.*, 2018ab; 2019ab). Previous studies have investigated the influence of the rubber particle properties (e.g. shapes, size, orientation) on the deformation (i.e. mainly compressibility) of the rubber-soil mixtures (e.g. Edil and Bosscher, 1994; Rao and Dutta, 2006; Lee *et al.*, 2007, 2010, Fonseca *et al.*, 2019; Sheikh *et al.*, 2012). These studies show that inter-particle sliding, grain rearrangement and distortion, as well as void-filling capacity of individual rubber particles contribute as key factors to the deformation mechanisms of rubber-soil mixtures. In contrast, for mixtures having much larger rubber particles (e.g. rubber chips and shredded rubber) bending and reorientation can be additional influential factors.

Generally, the addition of rubber will increase the compressibility of the mixture regardless of the size and shape of the blended rubber particles, but when the size of rubber particles is comparable to that of the rigid particles in the mixture, the geometry of the rubber particles have less influence on the overall deformation behaviour (Kim and Santamarina, 2008). Despite these findings, there is very limited research into how the amount of RC (R_b%) will affect the permanent strain rate ($\dot{\varepsilon}_p$) of mixtures subjected to repeated loading, or how R_b% will affect the deformation mechanism under large number of cyclic loading. It is therefore imperative to investigate $\dot{\varepsilon}_p$ to gain further insight into the deformation mechanism of rubber-soil/waste mixtures used in dynamic projects (i.e. highway pavements and railways), and to facilitate future road and track design.

The objective of this paper is to follow up the previous work conducted by the authors, (i.e Indraratna *et al.* 2017 and Qi *et al.* 2018a) to investigate the effect of R_b% and maximum cyclic deviator stresses ($q_{cyc,max}$) on $\dot{\varepsilon}_p$ and further on the deformation mechanism associated with the SFS+CW+RC mixtures subjected to repeated loading. In the SFS+CW+RC mixture, SFS (specific gravity 3.43) is a granulated by-product from steel industry with high shear strength and high abrasion and impact resistance; CW (specific gravity 2.11) is the commonest form of coal refuse from coal mining, and CW aggregates have less shear strength than conventional rockfill (base) materials and they are usually composed of both angular and flaky grains with a high potential for degradation; while RC (specific gravity 1.15) are shredded granular particles from waste tyres with high elasticity, and they are also highly deformable., The data from a series of consolidated drained cyclic triaxial tests on saturated SFS+CW+RC mixtures (SFS:CW=7:3, with $R_b\% = 0$, 10, 20, 30, and 40 % blended by weight) by Qi *et al.* (2018a) is considered here. All particles of RC, SFS and CW were sieved and mixed to the same particle size distribution as per the typical standards for subballast materials in Australian tracks as described by Indraratna *et al.* (2017) to avoid any overly influence of rubber particle size on the geotechnical properties of the mixtures. All the test specimens were prepared with the optimum moisture content and compacted to 95% of their maximum dry density. The effective confining pressures applied were $\sigma'_3 = 10, 40, \text{and } 70\ kPa$, and the cyclic stress ratio (CSR=$\frac{q_{cyc,max}}{2\sigma'_3}$) equals to 0.4 and 0.8. Further details of sample preparation and test procedures can be found elsewhere (Indraratna *et al.*, 2017; Qi *et al.*, 2018a). To further verify the empirical relationship derived from this study for RC-waste mixtures, two sets of cyclic triaxial test data from previous studies (e.g. Saberian *et al.,* 2018 and Tawk *et al.*, 2021) on recycled concrete aggregate (RCA) and RC mixtures (RCA+RC) and CW+RC mixtures are also adopted in the current study.

The influence of R_b *and q on* $\dot{\varepsilon}_p$

Fig.1 illustrates how $\dot{\varepsilon}_p$ evolves with the number of loading cycles (N) for the SFS+CW+RC mixture and the recycled concrete aggregate (RCA)+RC mixtures tested by Saberian *et al.* (2018). Note that the relationship of $\dot{\varepsilon}_p$ with N can be represented by a power function which is commonly used by other studies for granular materials (e.g. Monismith *et al.*, 1975; Li and Selig, 1996):

$$\dot{\varepsilon_p} = \beta \cdot N^{\alpha} \quad (1)$$

where N is the number of loading cycles; α is the slope of the permanent axial strain rate line in $\log \dot{\varepsilon_p} - \log N$ space, β is the $\dot{\varepsilon}_p$ (the initial vertical strain rate) when N=1. α and β are the parameters to reflect the influence of the type and condition of the soil and stress state. Note that a very good correlation can be noticed between the power fitting curves and the test data with R^2 over 0.97 for all conditions (Fig. 1).

From Fig. 1, it can be seen that when R_b% increases, $\dot{\varepsilon_p}$ plots higher for the same loading cycle, and the permanent axial strain rate line (PASRL) moves slightly anti-clockwise in $\dot{\varepsilon_p} - N$ space, which can also be reflected by the value of α which is the slope of PASRL as presented in Table 1, where the value of α increases with the increasing R_b (%) suggesting that the PASRL inclines upwards. This indicates that when an increased amount of RC is included, the reduction in $\dot{\varepsilon}_p$ with N is slower and thereby the vertical deformation is harder to achieve a constant value. This is understandable because as more RC is included, the mixture becomes less dense under the same compaction effort (Indraratna *et al.*, 2017; 2019), which induces a higher densification rate under cyclic loading. When increasing the rubber content from 0 to 40%, the skeleton of the mixture will transform from rigid particles (SFS and CW) to a softer matrix (reduced stiffness), as the rubber particles have lesser stiffness and higher compressibility than the CW and SFS aggregates. Therefore, it is expected that the rubber-blended matrix will transform from a traditional rigid granular material to a rubber-like behaviour (increased ductility) and continue to deform over the testing period, especially under higher vertical loads. The authors have shown earlier that this rubber-like transformation becomes significant when R_b =15-20% by mass (33-38% by volume) for the current particle gradation of the SFS+CW+RC mixtures (Qi *et al.*, 2018a). This observation is certainly in line with the results obtained for the sand-rubber mixtures studied by Lee *et al.*, (2007) and Kim and Santamarina (2008). Comparing with SFS+CW+RC matrix in the present study, this phenomenon is more obvious for RCA+RC mixtures even though the addition of RC is within a very small range ($\leq 2\%$). This is because the sensitivity of the influence of RC on parameter α is affected by the materials mixed with RC (i.e. SFS+CW and RCA). Since SFS and CW are different with RCA, the slope inclination of PASRL varies. Note that the increase in $q_{cyc,max}$ enlarges the difference of $\dot{\varepsilon}_p$ for waste mixtures having different $R_b\%$ at a certain cycle (Fig. 1a-c).

The influence of $q_{cyc,max}$ on $\dot{\varepsilon}_p$ can be clearly seen in Fig. 2, where the PASRL for SFS+CW+RC mixtures with $R_b = 10$ (%) under different values of $q_{cyc,max}$ are provided. At a certain number of cycle, $\dot{\varepsilon}_p$ increases as $q_{cyc,max}$ increases suggesting that higher axial loads can accelerate the accumulation of plastic deformation; however, the PASRL appears to be parallel, which indicates that $q_{cyc,max}$ has a negligible effect on the parameter α. This result is in conformity with previous studies on granular materials where the parameter α can be considered to be mainly represented by the type and physical condition of the material, rather than the loading conditions (Brown, 1974; Li and Selig, 1996). Given that all the SFS+CW+RC mixtures have been prepared under the same conditions but by only changing $R_b\%$, the parameter α can be represented in a linear relationship (Fig. 3) for $0 < R_b < 40$ (%), thus:

$$\alpha = m \cdot R_b + n \quad (2)$$

where *m* and *n* are empirical coefficients. This linear relationship is also suitable for RCA+RC mixtures, as shown in Fig. 3, but for a much narrower range of RC. A previous study by Tawk et al. (2021) on CW+RC mixtures with $0 < R_b < 15$ (%) tested under $q_{cyc,max} = 100\ kPa$ is also considered here, and it is found that Eq. (2) is capable of expressing adequately the relationship between α and R_b of the mixtures.

To better validate the proposed empirical relationships for α and β in this study, the available test data has been divided into two groups, i.e. Group A (for parameter calibrations) and Group B (for Validation), as shown in Table 1. The values of parameters m and n (Table 2) are obtained through best-fit regression using data in Group A, as shown in Fig. 3. Plotting the independent test data of Group B in Figure 3 shows that these points also fit the linear relationship proposed in Equation (2).

The parameter β which controls the initial $\dot{\varepsilon}_p$ of the materials is influenced by $R_b\%$ and $q_{cyc,max}$, as shown in Fig. 4a, where β is found to have a well-fitted logarithm relationship with $R_b\%$ ($R^2 > 0.95$):

$$\beta = A \cdot \ln(R_b + 1) + B \quad (3)$$

where A and B are calibration parameters related with $q_{cyc,max}$ based on data in Group A. Parameters A and B are then examined to have a linear relationship with $q_{cyc,max}$ for SFS+CW+RC mixtures (Fig. 4b):

$$A = A_1 \cdot q_{cyc,max} + A_2 \tag{4}$$

$$B = B_1 \cdot q_{cyc,max} + B_2 \tag{5}$$

where A_1, A_2, B_1, and B_2 are empirical coefficients. Therefore, by substituting Eqs. (4-5) into Eq. (3), the relationship between β with $R_b\%$ and $q_{cyc,max}$ can be represented by Eq. (6), as plotted in Fig. 5:

$$\beta = (A_1 q_{cyc,max} + A_2) \cdot \ln(R_b + 1) + (B_1 q_{cyc,max} + B_2) \tag{6}$$

Note that the value of β increases with $R_b\%$ and $q_{cyc,max}$ for the SFS+CW+RC mixtures. For RCA+RC mixtures (Saberian *et al.*, 2018) and CW+RC mixtures (Tawk *et al.,* 2021), as the data for different $q_{cyc,max}$ is not available, only the influence of $R_b\%$ on β is incorporated through Eq. (3), as plotted in Fig. 4a. Independent data from Group B are also shown in Fig. 4a and Fig. 5 for validation, where a good match can be observed. The values of all the calibration parameters are given in Table 2.

Substituting Eqs. (2) and (6) into Eq. (1), the PASRL can be obtained as:

$$\dot{\varepsilon_p} = \left[(A_1 q_{cyc,max} + A_2) \cdot \ln(R_b + 1) + (B_1 q_{cyc,max} + B_2)\right] \cdot N^{m \cdot R_b + n} \tag{7}$$

Fig. 6 shows that the predictions obtained by the empirical model (Eq. 7) match well with the test data from both Group A and Group B for SFS+CW+RC mixtures (Fig. 6ab), RCA+RC mixtures (Fig. 6c), and CW+RC mixtures (Fig. 6d).

There are discrepancies between the fitting curves for SFS+CW+RC mixtures (present study), CW+RC mixtures (Tawk *et al.,* 2021), and the RCA+RC mixtures (Saberian *et al.*, 2018) shown in Fig. 3 and Fig. 4a. The trend of best-fit matching curves for SFS+CW+RC mixtures is rather similar to the CW+RC mixtures, hence, SFS seems to have less influence compared to the more pronounced response attributed to CW and RC. However, it is noteworthy that the discrepancy of the fitting curves becomes more pronounced when the waste mining materials are replaced by RCA. This is most likely due to the difference in hardness between the blended materials with RC, such as CW (crushable and compressible) and SFS (high strength with good particle interlocking) compared to the more rigid and less crushable RCA (recycled concrete aggregates in Saberian *et al.*, 2018). These different waste materials can influence the sensitivity of the effect induced by the added rubber. For instance, PASRL rotates anti-clockwise much more obviously for RCA+RC mixtures than for SFS+CW+RC mixtures as

R_b% increases, as shown in Fig. 1. Since this paper is focused on the influence of RC, the influence of other materials is out of scope of this work.

Predictive permanent deformation mechanism

The failure pattern of the granular materials under static triaxial loading usually featured with a distinct shearing plane or bulging as the loading stress achieves to the peak deviator stress $q_{peak,static}$ (Sun *et al.*, 2015; Indraratna *et al.*, 2017). Unlike static failure, the material failure criterion under repeated loading with a constant $q_{cyc,max}$ is usually characterized by the accumulation of plastic deformation due to the absence of the $q_{peak,static}$ and the applied $q_{cyc,max}$ is generally relatively smaller than $q_{peak,static}$. Therefore, to better understand the deformation mechanism under repeated cyclic loading, the shakedown theory was introduced initially for engineering structures, then for pavement design, and later popularized for railway materials (Sharp and Booker, 1984; Sharp, 1985; Brett, 1987; Indraratna *et al.*, 2005; Tao *et al.*, 2010; Sun *et al.*, 2015; Qi and Indraratna, 2020). The basic assumption of the shakedown concept is that a test specimen or an engineering structure under repeated loading will eventually respond in a resilient (elastic/shakedown) manner or fail/collapse with extensive accumulated plastic deformation (Tao *et al.*, 2010). The criterion to discern the shakedown or failure was firstly proposed with a critical shakedown load/stress, and then prevailed by using the permanent strain rate (Werkmeister, 2005, 2006; Tao *et al.*, 2010).

Inspired by the shakedown theory (Werkmeister *et al.*, 2005; Tao *et al.*, 2010; Saberian *et al.*, 2018), the deformation response of SFS+CW+RC mixtures can be divided into the following categories (i.e. plastic shakedown, plastic creep and incremental collapse) based on the permanent axial strain behaviour in $\varepsilon_a - N$ space and the PASRL in $\dot{\varepsilon}_p - \varepsilon_a$ space up to 50,000 cycles shown in Fig. 7, by which most traditional subballast (granular) materials were found to achieve a stable deformation phase (Indraratna *et al.*, 2014; Bian *et al.*, 2016; Pirozzolo *et al.*, 2017).

Range A: Plastic shakedown, where the applied cyclic load is less than that required to induce the failure after the incremental accumulation of permanent deformation, and the material achieve a long-term steady state with insignificant permanent axial strain rate and hence ignorable accumulation of plastic strain for a finite number of loading cycles (here refers to 50,000 cycles), as shown in Fig. 7(a-b). This occurs (i) when SFS+CW+RC mixtures ($R_b \leq 40\%$) are tested at a lower $q_{cyc,max}$ (e.g. 16 kPa) or (ii) when R_b < 20%, as shown in Fig. 7(c-h), whereby the vertical deformation of the mixtures rapidly stabilizes before 1000 loading cycles (Fig. 7c-e) and $\dot{\varepsilon}_p$ decreases to a very small level (<10^{-8}) before the end of the test (N=50,000; Fig. 7f-h). It can be easily understood that all the SFS+CW+RC mixtures with $R_b \leq 40\,(\%)$ can achieve the plastic shakedown under a much smaller $q_{cyc,max}$ (e.g. 16 kPa) comparing to their peak deviator stress under static loading which can be 80-160 kPa (Qi *et al.*, 2019a). Moreover, when $R_b\%$ is within a low range (less than 20%), the waste mixtures can also achieve plastic shakedown even with a high $q_{cyc,max}$ (e.g. 112 kPa). This can be attributed to the relatively high stiffness of the SFS+CW+RC mixture having a low $R_b\%\,(<20\%)$ (Qi *et al.*, 2018a), and also a proper amount of added rubber (<20%) can effectively increase the energy absorbing property of the mixture to balance the finite amount input of the external energy without generating undesired elastic strain (Qi and Indraratna, 2020).

Range B: Plastic creep, where the specimen experiences a faster plastic strain accumulation than the specimen in **Range A** with the permanent strain rate gradually decreases to a relatively low level ($10^{-8} \leq \dot{\varepsilon}_p < 10^{-7}$) after a high number of loading cycles (Fig. 7a-b). Note that the permanent axial strain rate boundary between **Range A** and **B** is set to be $\dot{\varepsilon}_p = 10^{-8}$ as distinctly different deformation behaviour can be observed for SFS+CW+RC mixtures ending with $\dot{\varepsilon}_p > 10^{-8}$ and $\dot{\varepsilon}_p < 10^{-8}$ (Fig. 7), which is consistent with similar observations reported earlier by Tao *et al.*, (2010). The boundary of Range B (plastic creep) and range C (incremental collapse) is set as $\dot{\varepsilon}_p = 10^{-7}$/cycle, which is a typical common boundary for granular materials/mixtures as suggested in previous studies, e.g. Tao *et al.*, (2010) for blended recycled granular base materials (blended calcium sulfate, blast furnace slag, Class C fly ash, recycled asphalt pavement, foamed-asphalt), Saberian *et al.,* (2018) for recycled concrete aggregates and crushed rock mixed with rubber crumbs, and Werkmeister *et al.*, (2005) and Sun *et al.* (2015) for crushed rock aggregates. As there is no failure/collapse observed for the current waste mixtures with $R_b \leq 40\%$ under the test conditions reported in this study, $\dot{\varepsilon}_p = 10^{-7}$/cycle is adopted as the boundary of Range B and C which the authors consider to be reasonable. The plastic creep occurs for SFS+CW+RC mixtures having higher RC contents ($R_b > 20\%$) and subjected to a higher $q_{cyc,max}$ (e.g. $q_{cyc,max} \geq 64\ kPa$) as shown in Fig. 7 (c-h), where the permanent axial strain continues to increase until the end of the test with $10^{-8} \leq \dot{\varepsilon}_p < 10^{-7}$ albeit an obvious reduction in $\dot{\varepsilon}_p$ is observed after 1000 cycles. Note that when both $R_b\%$ and $q_{cyc,max}$ increase, ε_a increases and the slope of PASRL inclines upwards, especially under higher values of $q_{cyc,max}$ (Fig. 7f-h). This indicates that a combination of

R_b% and $q_{cyc,max}$ with higher magnitudes will certainly accelerate the accumulation of permanent deformation of the waste mixture. Further, higher R_b% in the waste mixtures will end up with a looser specimen during specimen preparation (Indraratna *et al.*, 2017), hence taking a longer time for densification under cyclic loading, and the increased elasticity caused by a higher R_b% will induce instability in terms of displacement (Qi and Indraratna, 2020), thus preventing the specimen achieving plastic shakedown.

Range C: Incremental collapse. The typical description is that $\dot{\varepsilon}_p$ decreases very slowly or not at all to the end of the test ($\dot{\varepsilon}_p \geq 10^{-7}$), while the large plastic strain that accumulates rapidly causes early failure after a relatively low number of loading cycles. During the cyclic loading test on the SFS+CW+RC mixtures, no failure or collapse occurred due to the limited range of R_b% and $q_{cyc,max}$ tested in this study. Therefore, it is imperative to predict the permanent deformation response of the waste mixtures for a wider range of R_b% and $q_{cyc,max}$.

A large accumulation of permanent strain will induce a high risk of track failure, therefore the SFS+CW+RC mixture in Range A (plastic shakedown) is the most preferable to be used in railways. To facilitate future design when using SFS+CW+RC mixtures as a potential subballast, $\dot{\varepsilon}_p$ of waste mixtures with a broader range of R_b% and $q_{cyc,max}$ at loading cycle N=50,000 can be predicted using the empirical Eq. (7), as illustrated in Fig. 8. The $q_{cyc,max}$ is used up to 166 kPa to simulate the vertical load of a heavy haul train with a 30-tonne axle load (Indraratna *et al.*, 2014). The predictive permanent axial strain rate surface is divided into three parts (i.e. Range A, Range B and Range C) based on shakedown theory using the boundaries of $\dot{\varepsilon}_p = 10^{-7}$ and $\dot{\varepsilon}_p = 10^{-8}$. Note that under $q_{cyc,max} = 166\ kPa$, the waste mixture with $15.56\% < R_b\% < 62.22\%$ falls within Range B (plastic creep), while the mixtures having $R_b > 62.22\ (\%)$ will tend to collapse. Therefore, it is suggested that for a heavy haul track with axle loads over 30 tonnes, the amount of RC added to the subballast mixtures should be less than 15% by weight.

The proposed empirical model Eq. (7) is based on the test results of SFS+CW+RC mixtures with $R_b \leq 40\%$ and the particle sizes of the rubber crumbs being comparable to the sizes of other materials in the mixtures (i.e. SFS and CW). The model should not be applied for RC greater than 40% without exercising caution. It is also noteworthy that the effect of varying the rubber particle size and shape is not captured in the model. The purpose of the model predictions is to provide some guidance to practicing engineers, noting the inherent limitations of this empirical model. It is obvious that further validations will need to be conducted in the future research for significantly higher rubber contents over a wider range of strain rates applied to a greater range of cyclic loading conditions.

Conclusions

This study was focused on the effect of rubber contents and loading conditions on the cyclic permanent deformation behaviour of a waste granular matrix containing coal wash (CW) and steel furnace slag (SFS) based on a series of cyclic loading tests on SFS+CW+RC mixtures with $R_b\% \leq 40\%$ and $q_{cyc,max} = 16 - 112\ kPa$). The following conclusions can be drawn from this study:

- The RC content ($R_b\%$) has a significant influence on the trend of the permanent axial strain rate line (PASRL) and the initial $\dot{\varepsilon}_p$, while $q_{cyc,max}$ mainly affects the initial $\dot{\varepsilon}_p$ of the waste mixture.
- The PASRL in the $\dot{\varepsilon}_p - \varepsilon_a$ space obtained from cyclic loading tests indicates that SFS+CW+RC mixtures can easily achieve plastic shakedown with a smaller $R_b\%$ (<20%) or under very low $q_{cyc,max}$ (e.g. 16 kPa), whereas waste mixtures with a greater value of $R_b\%$ (30-40%) and under higher $q_{cyc,max}$ (64-112 kPa) show plastic creep towards the end of the test.
- An empirical model was proposed for the permanent axial strain rate of SFS+CW+RC mixtures capturing the effects of $R_b\%$ and $q_{cyc,max}$. Independent sets of data of SFS+CW+RC mixtures from the current study and rubber-waste mixtures from previous studies (e.g. RCA+RC mixture from Saberian *et al.*, 2018 and CW+RC mixtures from Tawk *et al.*, 2021) have been used to validate the model, and the model prediction matches the test data very well. This indicates that this empirical model is able to predict the permanent vertical deformation behaviour of other RC-waste granular mixtures under repeated loading.
- The empirical model was extended to predict the $\dot{\varepsilon}_p$ of waste mixtures having a broader range of $R_b\%$ and $q_{cyc,max}$ up to 166 kPa (the pressure on top of the subballast under an axle load of 30 tonnes) to provide references for practical engineers. Based on the model prediction, it is recommended that the RC content in the SFS+CW+RC mixtures should be less than 15% for heavy haul trains with axle loads over 30 tonnes to avoid the risk of track failure due to excessive settlement.

It is noteworthy that the empirical model has some limitations given the range of rubber content tested in this study (< 40%), and the influence of RC that can vary according to the type of other waste materials in the mixture (e.g. properties of CW and SFS can also change geographically). Moreover, different particle sizes and shapes in the matrix, and the cyclic loading characteristics can influence the rate and magnitude of accumulated deformations. Therefore, the proposed empirical model when used beyond the tested conditions and material characteristics will require caution to be exercised.

Acknowledgements

The authors would like to acknowledge the financial assistance provided by the Australian Research Council Discovery Project (ARC-DP; project ID: DP180101916) and ARC Industry Transformation Training Centre for Advanced Rail Track Technologies (ITTC-Rail, project ID: IC170100006).

References

Bian, X., Jiang, J., Jin, W., Sun, D., Li, W. and Li, X. (2016). Cyclic and postcyclic triaxial testing of ballast and subballast. *Journal of Materials in Civil Engineering* **28**(7): 04016032.

Brett, J. (1987). Stability and shakedown in pavement roughness change with age. New Zealand Roading Symposium, 1987, Wellington, New Zealand (volume 4).

Brown, S. (1974). Repeated load testing of a granular material. *Journal of Geotechnical and Geoenvironmental Engineering* **100**(Proc. Paper 10684).

Cerni, G., Cardone, F. and Bocci, M. (2012). Permanent deformation behaviour of unbound recycled mixtures. *Construction and Building Materials* **37**: 573-580.

Edil, T.B. and Bosscher, P.J., (1994). Engineering properties of tire chips and soil mixtures. *Geotechnical testing journal* **17**(4): 453-464.

Esmaeili, M., Zakeri, J. A., Ebrahimi, H. and Khadem Sameni, M. (2016). Experimental study on dynamic properties of railway ballast mixed with tire derived aggregate by modal shaker test. *Advances in Mechanical Engineering* **8**(5): 1687814016640245.

Fathali, M., Nejad, F. M. and Esmaeili, M. (2016). Influence of tire-derived aggregates on the properties of railway ballast material. *Journal of materials in civil engineering* **29**(1): 04016177.

Fonseca, J., Bernal-Sanchez, J., Riaz, A., Barreto, D., McDougall, J., Miranda-Manzanares, Marinelli, M., A. and Dimitriadi, V. (2019). Particle-Scale Interactions and Energy Dissipation Mechanisms in Sand-Rubber Mixtures. *Géotechnique Letters* **9**(4):1-6. DOI: 10.1680/jgele.18.00221.

Fu, R., Coop, M. and Li, X. (2014). The mechanics of a compressive sand mixed with tyre rubber. *Géotechnique Letters* **4**(3): 238-243.

Indraratna, B., Biabani, M. M. and Nimbalkar, S. (2014). Behavior of geocell-reinforced subballast subjected to cyclic loading in plane-strain condition. *Journal of Geotechnical and Geoenvironmental Engineering* **141**(1): 04014081.

Indraratna, B., Lackenby, J. and Christie, D. (2005). Effect of confining pressure on the degradation of ballast under cyclic loading. *Géotechnique* **55**(4): 325-328.

Indraratna, B., Qi, Y. and Heitor, A. (2017). Evaluating the properties of mixtures of steel furnace slag, coal wash, and rubber crumbs used as subballast. *Journal of Materials in Civil Engineering* **30**(1): 04017251.

Indraratna, B., Rujikiatkamjorn, C., Tawk, M. and Heitor, A. (2019). Compaction, degradation and deformation characteristics of an energy absorbing matrix. *Transportation Geotechnics* **19**: 74-83.

Kim, H.K and Santamarina, J.C. (2008). Sand-Rubber Mixtures (Large Rubber Chips). *Canadian Geotechnical Journal* **45**(10): 1457-1466. DOI: 10.1139/T08-070.

Lee, C., Truong, Q.H., Lee, W. and Lee J.S. (2010). Characteristics of Rubber-Sand Particle Mixtures according to Size Ratio. *Journal of Materials in Civil Engineering* **22**(4): 323-331. DOI: 10.1061/(ASCE)MT.1943-5533.0000027.

Lee, J.S., Dodds, J. and Santamarina, J.C. (2007). Behavior of Rigid-Soft Particle Mixtures. *Journal of Materials in Civil Engineering* **19**(2):179-184. DOI: 10.1061/(ASCE) 0899-1561(2007)19:2(179).

Li, D. and Selig, E. T. (1996). Cumulative plastic deformation for fine-grained subgrade soils. *Journal of geotechnical engineering* **122**(12): 1006-1013.

Madhusudhan, B., Boominathan, A. and Banerjee, S. (2017). Static and large-strain dynamic properties of sand–rubber tire shred mixtures. *Journal of Materials in Civil Engineering* **29**(10): 04017165.

Madhusudhan, B., Boominathan, A. and Banerjee, S. (2019a). Engineering properties of sand–rubber tire shred mixtures. *International Journal of Geotechnical Engineering*: 1-17.

Madhusudhan, B., Boominathan, A. and Banerjee, S. (2019b). Factors Affecting Strength and Stiffness of Dry Sand-Rubber Tire Shred Mixtures. *Geotechnical and Geological Engineering* **37**(4): 2763-2780.

Mashiri, M., Vinod, J., Sheikh, M. N. and Tsang, H.-H. (2015). Shear strength and dilatancy behaviour of sand–tyre chip mixtures. *Soils and Foundations* **55**(3): 517-528.

Monismith, C. L., Ogawa, N. and Freeme, C. (1975). Permanent deformation characteristics of subgrade soils due to repeated loading. *Transportation Research Record*(537).

Pirozzolo, L., Sol-Sánchez, M., Moreno-Navarro, F., Martínez-Montes, G. and Rubio-Gámez, M. (2017). Evaluation of bituminous sub-ballast manufactured at low temperatures as an alternative for the construction of more sustainable railway structures. *Materiales de Construcción* **67**(327): 128.

Platzer, A., Rouhanifar, S., Richard, P., Cazacliu, B. and Ibraim, E. (2018). Sand-Rubber Mixtures Undergoing Isotropic Loading: Derivation and Experimental Probing of a Physical Model. *Granular Matter* **20**(4): 1-10. DOI: 10.1007/s10035-018-0853- 7.

Qi, Y. and Indraratna, B. (2020). Energy-Based Approach to Assess the Performance of a Granular Matrix Consisting of Recycled Rubber, Steel-Furnace Slag, and Coal Wash. *Journal of Materials in Civil Engineering* **32**(7): 04020169.

Qi, Y., Indraratna, B. and Coop, M. R. (2019a). Predicted Behavior of Saturated Granular Waste Blended with Rubber Crumbs. *International Journal of Geomechanics* **19**(8): 04019079.

Qi, Y., Indraratna, B., Heitor, A. and Vinod, J. (2019b). The influence of rubber crumbs on the energy absorbing property of waste mixtures. Geotechnics for Transportation Infrastructure. Sundaram R., S. J., Havanagi V. Singapore, Springer. **29:** 271-281.

Qi, Y., Indraratna, B., Heitor, A. and Vinod, J. S. (2018a). Effect of rubber crumbs on the cyclic behavior of steel furnace slag and coal wash mixtures. *Journal of Geotechnical and Geoenvironmental Engineering* **144**(2): 04017107.

Qi, Y., Indraratna, B. and Vinod, J. S. (2018b). Behavior of Steel Furnace Slag, Coal Wash, and Rubber Crumb Mixtures with Special Relevance to Stress–Dilatancy Relation. *Journal of Materials in Civil Engineering* **30**(11): 04018276.

Rao, G.V. and Dutta, R.K., (2006). Compressibility and strength behaviour of sand–tyre chip mixtures. *Geotechnical & Geological Engineering* **24**(3): 711-724.

Saberian, M., Li, J., Nguyen, B. and Wang, G. (2018). Permanent deformation behaviour of pavement base and subbase containing recycle concrete aggregate, coarse and fine crumb rubber. *Construction and Building Materials* **178**: 51-58.

Sharp, R. (1985). Pavement design based on shakedown analysis. *Transp. Res. Rec.* **1022**: 99–107.

Sharp, R. and Booker, J. (1984). Shakedown of pavements under moving surface loads. *J. Transp. Eng.* **110** (1): 1–14.

Sheikh, M.N., Mashiri, M.S., Vinod, J.S. and Tsang, H.H. (2012). Shear and Compressibility Behaviours of Sand-Tyre Crumb Mixtures. *Journal of Materials in Civil Engineering* **25**(10). DOI: 10.1061/(ASCE)MT.1943-5533.0000696.

Sol-Sánchez, M., Moreno-Navarro, F. and Rubio-Gámez, M. C. (2015). The use of elastic elements in railway tracks: A state of the art review. *Construction and building materials* **75**: 293-305.

Sun, Q. D., Indraratna, B. and Nimbalkar, S. (2015). Deformation and degradation mechanisms of railway ballast under high frequency cyclic loading. *Journal of Geotechnical and Geoenvironmental Engineering* **142**(1): 04015056.

Tao, M., Mohammad, L. N., Nazzal, M. D., Zhang, Z. and Wu, Z. (2010). Application of shakedown theory in characterizing traditional and recycled pavement base materials. *Journal of Transportation Engineering* **136**(3): 214-222.

Tawk, M., Qi, Y., Indraratna, B., Rujikiatkamjorn, C. and Heitor, A., (2021). Behavior of a Mixture of Coal Wash and Rubber Crumbs under Cyclic Loading. *Journal of Materials in Civil Engineering*, **33**(5): 04021054.

Tseng, K.-H. and Lytton, R. L. (1989). Prediction of permanent deformation in flexible pavement materials. Implication of aggregates in the design, construction, and performance of flexible pavements, ASTM International.

Werkmeister, S. (2006). Shakedown analysis of unbound granular materials using accelerated pavement test results from New Zealand's CAPTIF facility. *Geotechnical Specical Publications* **154** ASCE, Reston: 220-228.

Werkmeister, S., Dawson, A. R. and Wellner, F. (2005). Permanent deformation behaviour of granular materials. *Road materials and pavement design* **6**(1): 31-51.

Wichtmann, T., Niemunis, A. and Triantafyllidis, T. (2007). Strain accumulation in sand due to cyclic loading: drained cyclic tests with triaxial extension. *Soil Dynamics and Earthquake Engineering* **27**(1): 42-48.

Youwai, S. and Bergado, D. T. (2003). Strength and deformation characteristics of shredded rubber tire sand mixtures. *Canadian Geotechnical Journal* **40**(2): 254-264.

Figure captain

Fig. 1 Permanent axial strain rate for SFS+CW+RC (present study) and RCA+RC mixtures tested by Saberian *et al.* (2018)

Fig. 2 Permanent axial strain rate for SFS+CW+RC mixtures with $R_b = 10\ (\%)$ under different cyclic deviator stresses

Fig. 3 The relationship of parameter α and RC contents

Fig. 4 Calibration coefficients for parameter β

Fig. 5 The relationship of parameter β, RC contents and cyclic deviator stress

Fig. 6 Test data and model prediction of Equation (7)

Fig. 7 (a-b) Permanent deformation response of SFS+CW+RC mixtures based on shakedown theory; (c-e) Permanent axial strain versus number of loading cycles (modified after Qi *et al.*, 2018); (f-h) permanent axial strain rate versus permanent axial strain for SFS+CW+RC mixtures

Fig. 8 Predictive permanent axial strain rate at N=50,000 cycles varying with cyclic deviator stress and RC contents

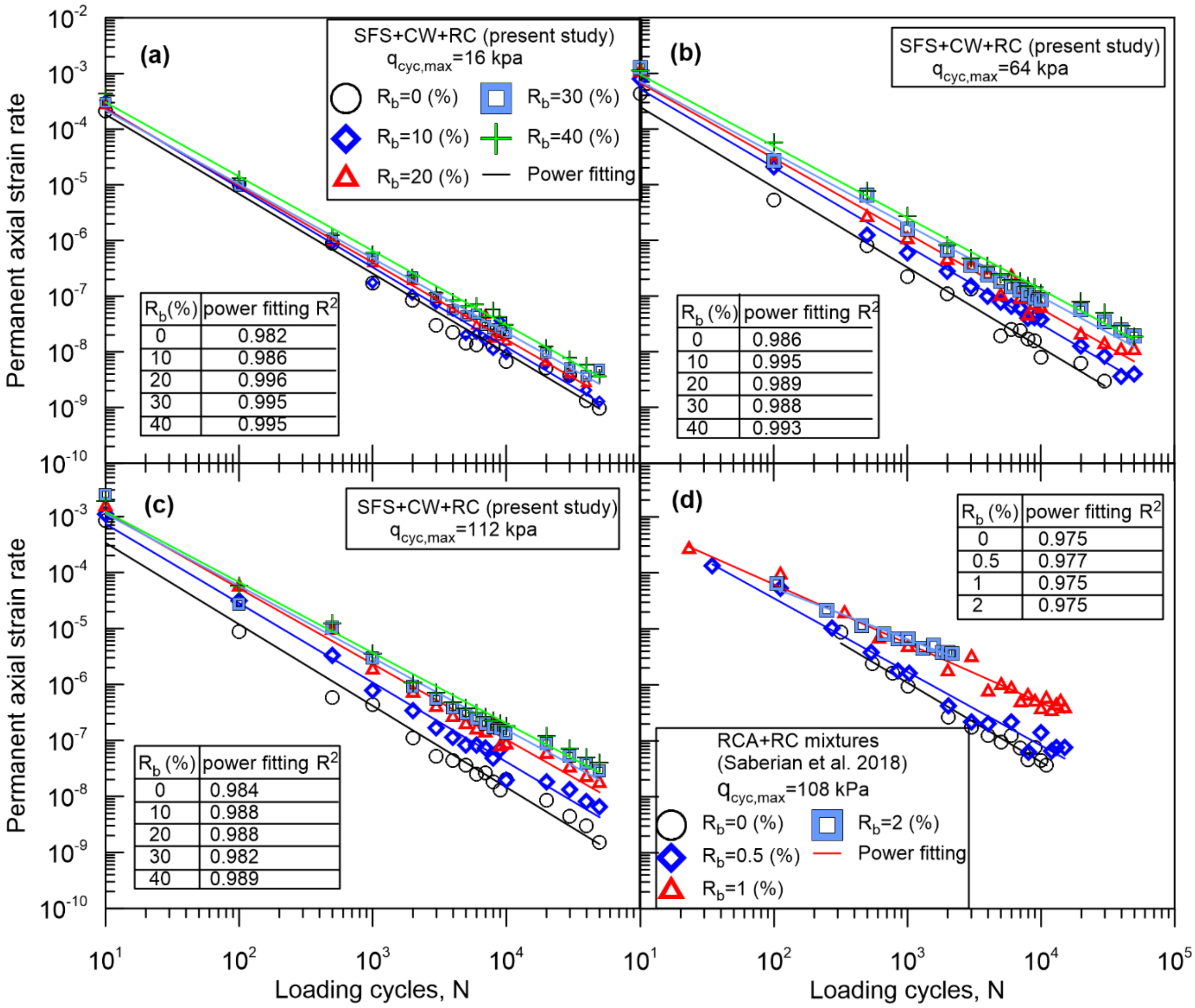

Fig. 1 Permanent axial strain rate for SFS+CW+RC (present study) and RCA+RC mixtures tested by Saberian *et al.* (2018)

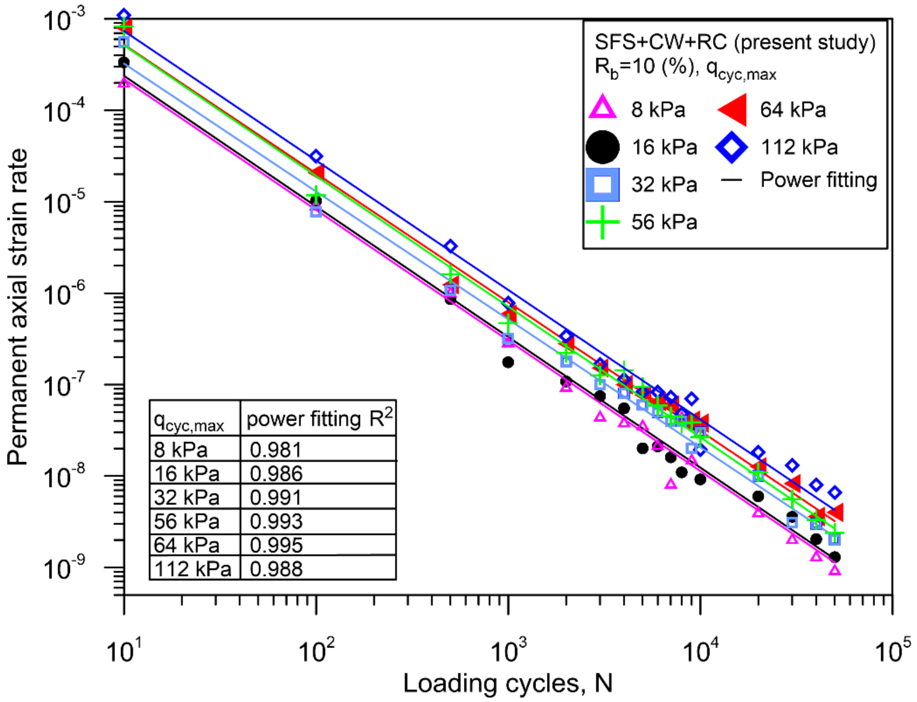

Fig. 2 Permanent axial strain rate for SFS+CW+RC mixtures with $R_b = 10$ (%) under different cyclic deviator stresses

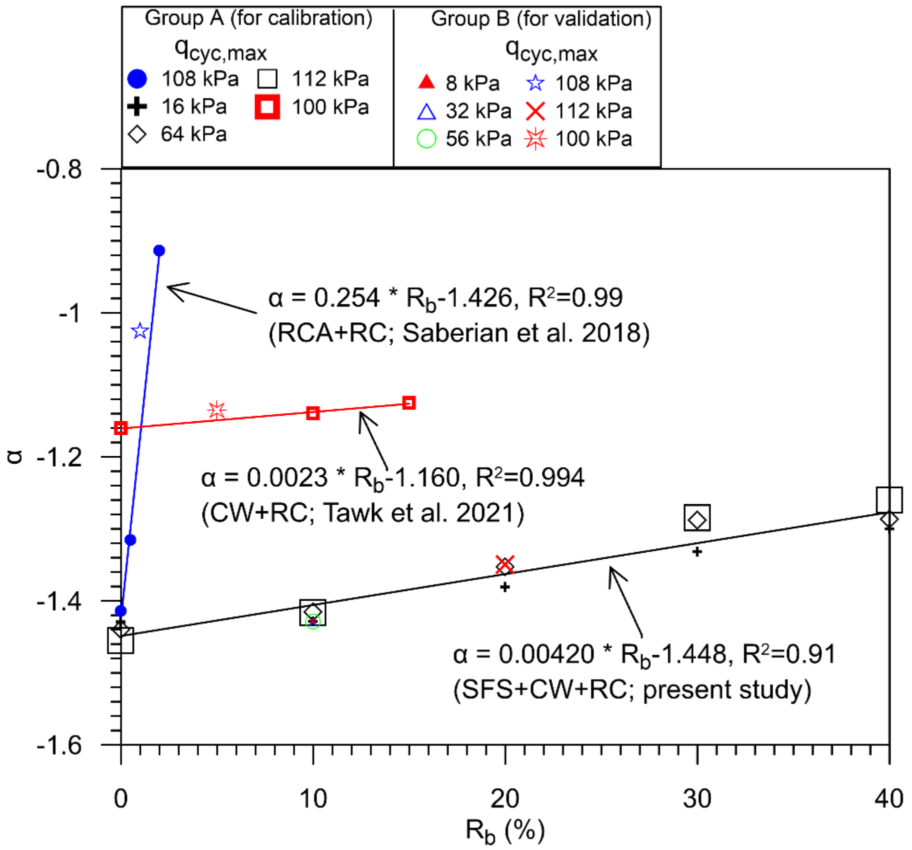

Fig. 3 The relationship of parameter α and RC contents

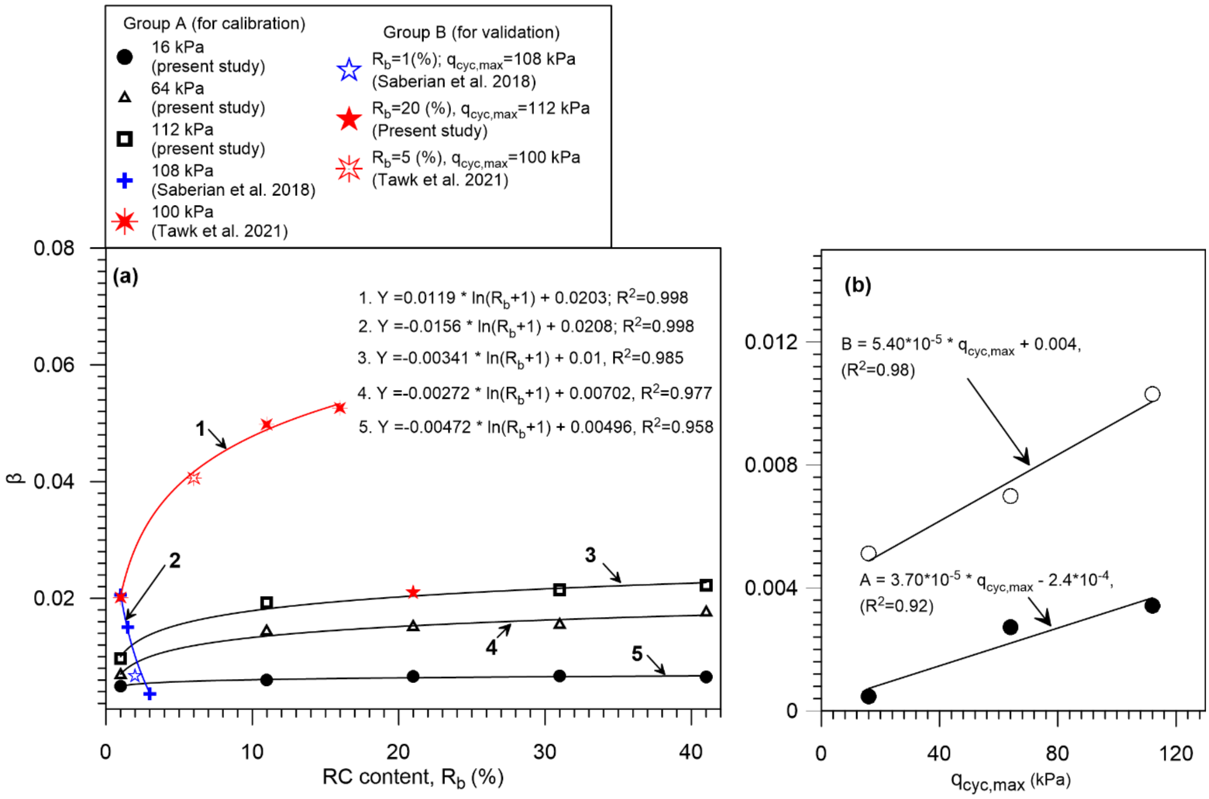

Fig. 4 Calibration coefficients for parameter β

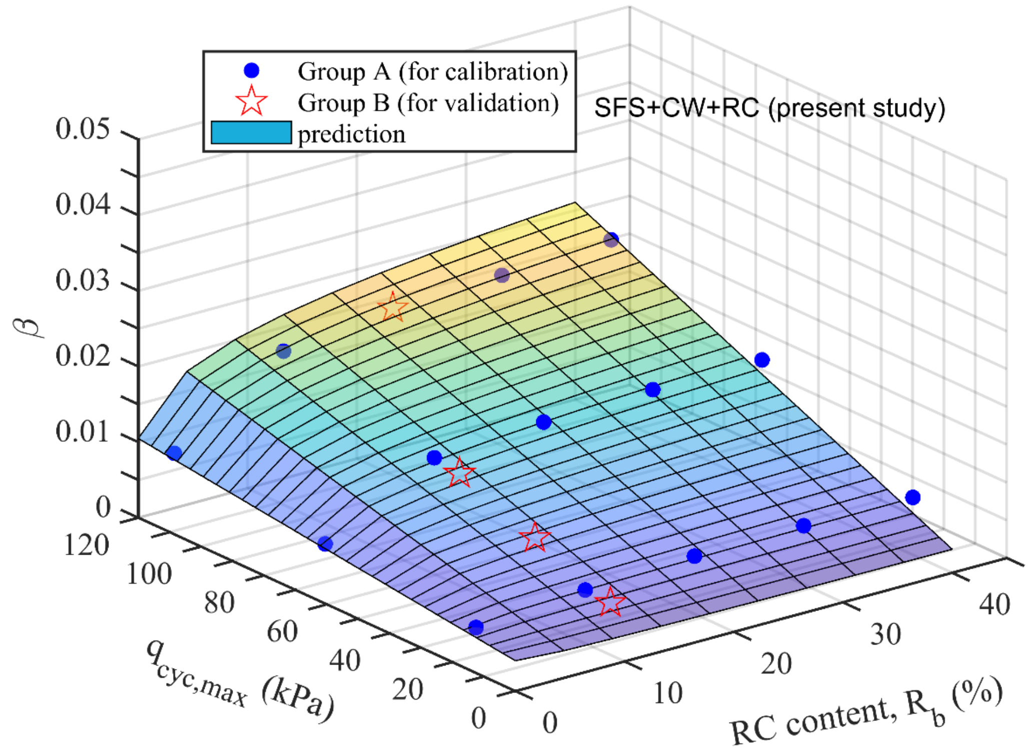

Fig. 5 The relationship of parameter β, RC contents and cyclic deviator stress

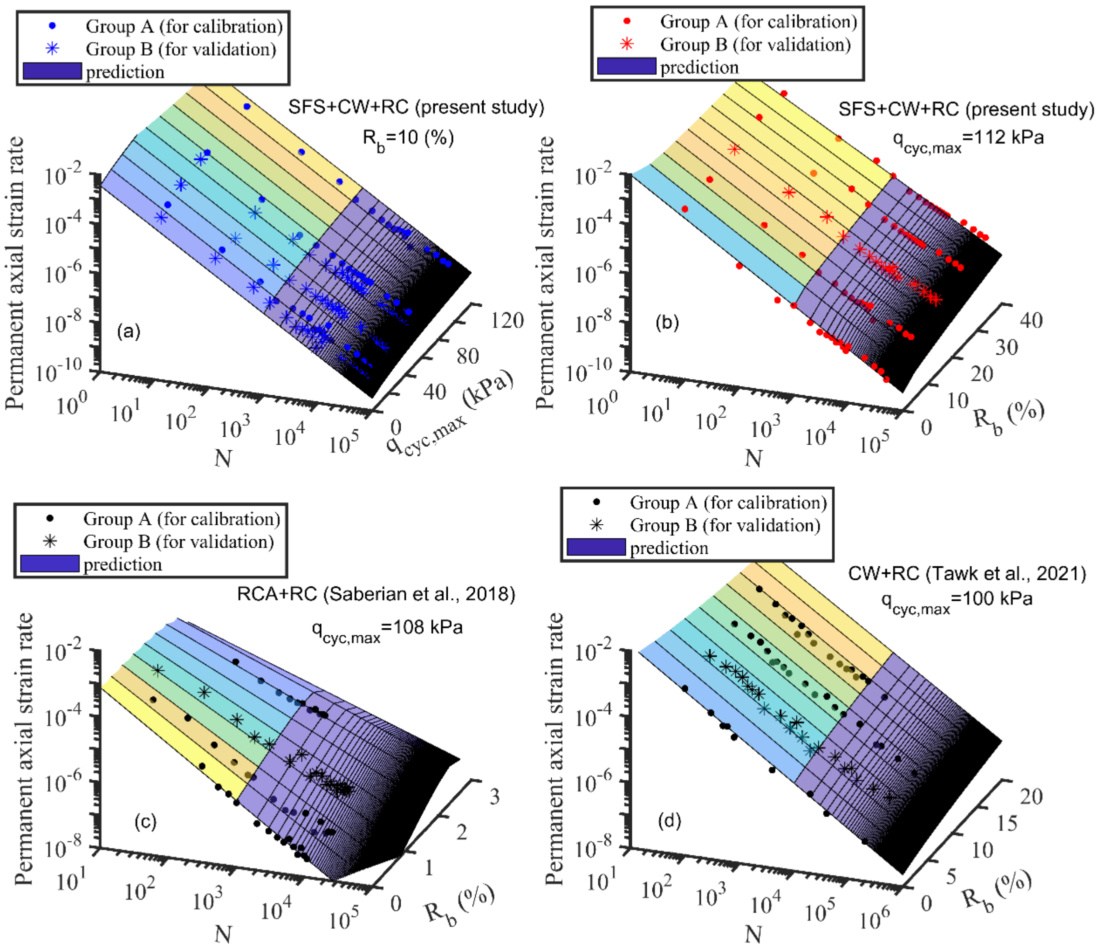

Fig. 6 Test data and model prediction of Equation (7)

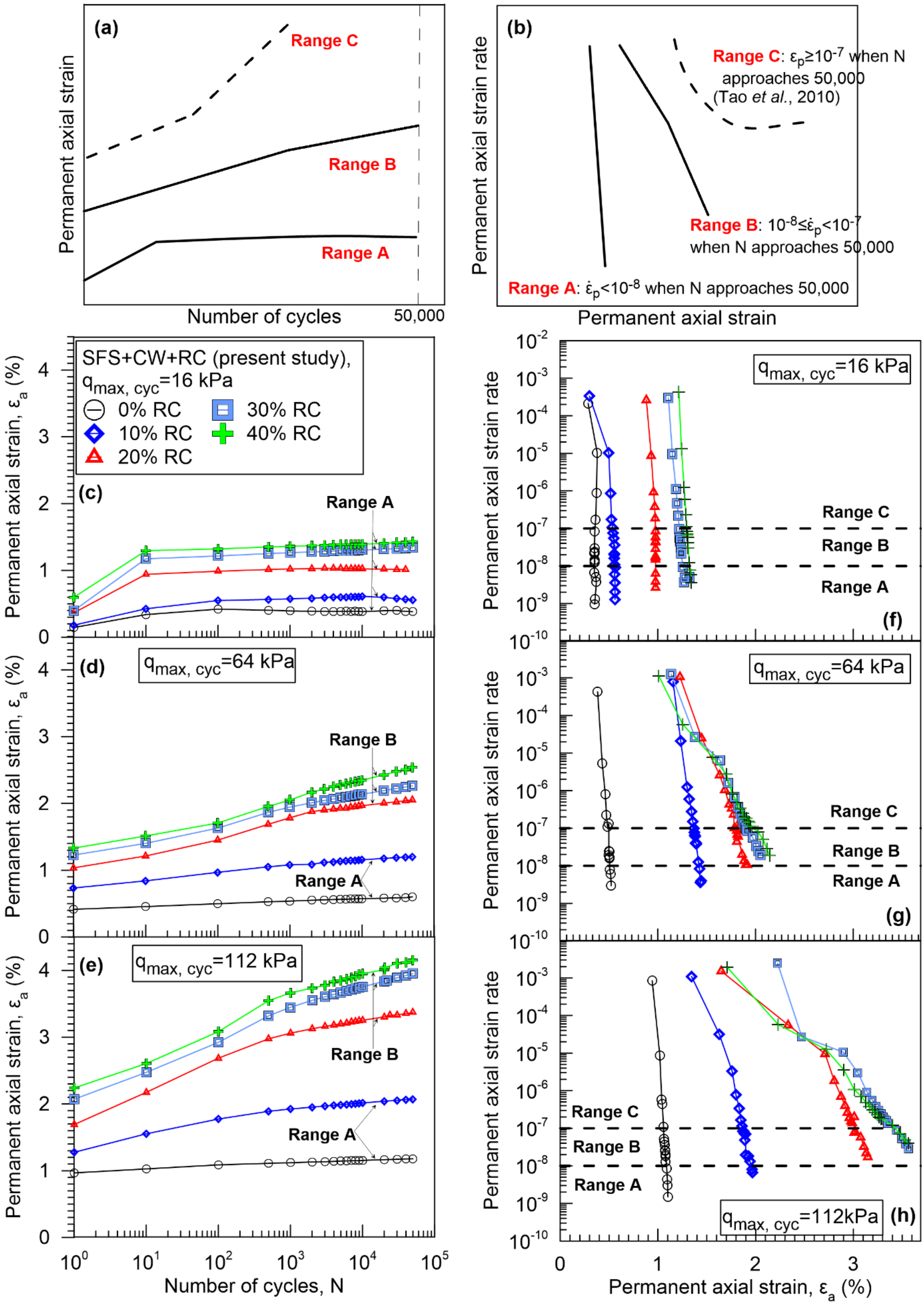

472

473 Fig. 7 (a-b) Permanent deformation response of SFS+CW+RC mixtures based on shakedown theory;
474 (c-e) Permanent axial strain versus number of loading cycles (modified after Qi *et al.*, 2018); (f-h)
475 permanent axial strain rate versus permanent axial strain for SFS+CW+RC mixtures

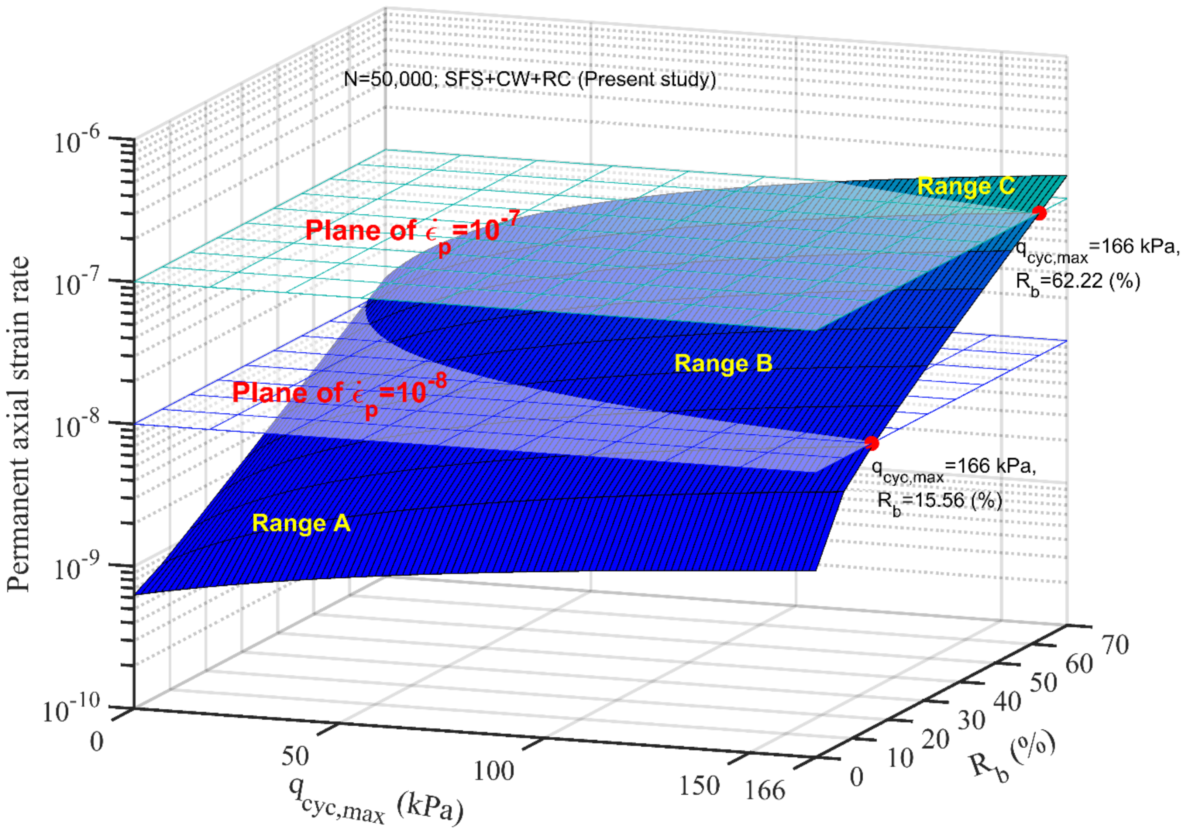

476

477 Fig. 8 Predictive permanent axial strain rate at N=50,000 cycles varying with cyclic deviator stress and
478 RC contents

Table list

Table 1 Value of α and β for Equation (1)

SFS+CW+RC (present study)							**RCA+RC (Saberian *et al.*, 2018)**		
R_b (%)	$q_{cyc,max} = 16$ kPa		$q_{cyc,max} = 64$ kPa		$q_{cyc,max} = 112$ kPa		R_b (%)	$q_{cyc,max} = 108$ kPa	
	α	β	α	β	α	β		α	β
0 (A)	-1.429	0.00495	-1.440	0.00683	-1.455	0.00966	0 (A)	-1.414	0.0206
10 (A)	-1.428	0.00640	-1.415	0.0143	-1.416	0.0192	0.5 (A)	-1.315	0.0150
20 (A,B)	-1.381	0.00557	-1.353	0.0151	-1.350	0.0210	1 (B)	-1.026	0.00667
30 (A)	-1.330	0.00668	-1.288	0.0155	-1.285	0.0215	2 (A)	-0.914	0.00358
40 (A)	-1.310	0.00653	-1.286	0.0175	-1.260	0.0222	**CW+RC (Tawk *et al.*, 2021)** $q_{cyc,max} = 100$ kPa		
R_b (%)	$q_{cyc,max} = 8$ kPa		$q_{cyc,max} = 32$ kPa		$q_{cyc,max} = 56$ kPa		0 (A)	-1.160	0.020167
	α	β	α	β	α	β	5 (B)	-1.135	0.040590
10 (B)	-1.428	0.00585	-1.430	0.00983	-1.429	0.0138	10 (A)	-1.139	0.049763
-	-	-	-	-	-	-	15 (A)	-1.125	0.052591

*where data in Group A is used for parameters calibration, and data in Group B is used for validation. For SFS+CW+RC mixtures with 20%RC, only the test data obtained under $q_{cyc,max} = 112$ kPa is in Group B, and those obtained under $q_{cyc,max} = 16, 64$ kPa are in Group A.

Table 2 Model parameters based on test data in Group A

Waste mixtures	m	n	A_1	A_2	B_1	B_2
SFS+CW+RC mixtures (present study)	0.00420	-1.448	3.69× 10^{-5}	-2.40× 10^{-4}	5.40× 10^{-5}	0.004
RCA+RC mixtures (Saberian *et al.*, 2018)	0.254	-1.426	A=-0.0156		B=0.0208	
CW+RC mixtures (Tawk *et al.*, 2021)	0.0023	-1.160	A=0.0119		B=0.0203	